**EURO:TUN 2013**
3rd International Conference on
Computational Methods in Tunneling and Subsurface Engineering
Ruhr University Bochum, 17-19 April 2013

# In-situ Measurement and Numerical Analysis on Tunnel Lining and Ground Behaviour due to Shield Excavation

**Takahiro Konda[1], Junichi Nagaya[1], Tadashi Hashimoto[1], Hossain M. Shahin[2] and Teruo Nakai[2]**
[1]Geo-Research Institute, Japan
[2]Nagoya Institute of Technology, Japan

## Abstract

In urban tunnelling, often construction is done under some constrained conditions. In this paper, the ground movement due to shield excavation is observed and some measurements of the first tunnel lining pressure and stress development due to the excavation of second shield tunnel close to the first tunnel are carried out. The influence of the construction loads due to shield tunnelling on the surrounding ground and nearby structures is discussed. Numerical analysis is also carried out with elasto-plastic constitutive model of soil in which the mechanical characteristic of ground material and the construction process are appropriately taken into consideration. Comparing the results of the analyses with the monitoring data, the behaviour of surrounding ground and existing structure due to shield excavation is investigated focusing on the influence of the construction loads. The finite element analyses are carried out with FEM tij-2D software using an elasto-plastic constitutive model of soils, named subloading $t_{ij}$ model. It is revealed that during the construction of the following tunnel loads acted on the lining of the preceding tunnel. The elasto-plastic FE analysis is able to explain these actual behaviours adequately that cannot be expressed by the analysis using the conventional stress release ratio.

**Keywords:** Shield tunnel, monitoring, numerical analysis, subloading $t_{ij}$ model, construction load

## 1 INTRODUCTION

In urban shield tunnelling, often construction is done at about 1m distance under some constrained conditions such as the limitation of the road width and the existence of the underground structures. In these neighbouring constructions, it is necessary to evaluate the influence and assess the safety of surrounding ground and existing structure due to shield excavation adequately. The calculation method with stress released ratio is usually used in Japan to predict the ground behaviour due to shield excavation. However, because ground movements are depended on some construction conditions, for example cutter face pressure, backfill grouting pressure, control position of shield machine and so on, ground deformation behaviours are different each construction steps.

In this paper, the ground movement due to shield excavation is observed and some measurements of the first tunnel lining pressure and stress development due to the excavation of second shield tunnel close to the first tunnel are carried out. The influence of the construction loads due to shield tunnelling on the surrounding ground and nearby structures is discussed. Numerical analysis is also carried out with elasto-plastic constitutive model of soil in which the mechanical characteristic of ground material and the construction process are appropriately taken into consideration. Comparing the results of the analyses with the monitoring data, the behaviour of surrounding ground and existing structure due to shield excavation is investigated focusing on the influence of the construction loads. The finite element analyses are carried out with FEM tij-2D software using an elasto-plastic constitutive model of soils, named subloading $t_{ij}$ model [2]. This constitutive model has already applied to some braced excavation problems [1] and tunnel excavation problems [3], and calculation results had good response to model test results.

## 2 SOILS CHARACTERISTICS AND CONSTRUCTION CONDITIONS

Figure 1 show the soil profile and installation position of monitoring apparatus in the target construction site of shield excavation. The specifications of tunnel lining and excavation conditions when the shield passes through the monitoring section are shown in Table 1. The monitoring section was set at the area which is very close the second tunnel, where the second shield tunnel is obliquely upward of the first tunnel with a distance of about 1,1m.

Holocene layer and Pleistocene layer exist from the ground surface to the place near this monitoring site. Holocene layer is composed of a fine sandy layer (Aus), soft clay layers (Amc1 and Amc2), a sand gravel layer (Amg) and a sandy layer with medium density (As). On the other hand, Pleistocene layer exist in the lower part of Holocene layer, and is composed of a stiff clay layers (Oc2), a dense gravel layer (Tg) and a dense sandy layer (Os2). Table 2 shows some characteristics of each layer.
The upper ground of the first tunnel is formed with Amc2 and Ams soft layers. Meanwhile, hard layer Oc2 and Tg exist in the lower side ground of the first tunnel. In contrast, dense sand gravel layer Amg exist in the upper ground of the second tunnel, and soft clay layer Amc2 exists at the lower ground of the second tunnel.
The vertical displacement above the first tunnel and the horizontal displacement along with the vertical distance beside the first tunnel due to shield excavation are measured. Moreover, to evaluate the influence of the construction loads on the first tunnel lining due to second shield excavation, first tunnel lining pressure and cross section force are monitored.

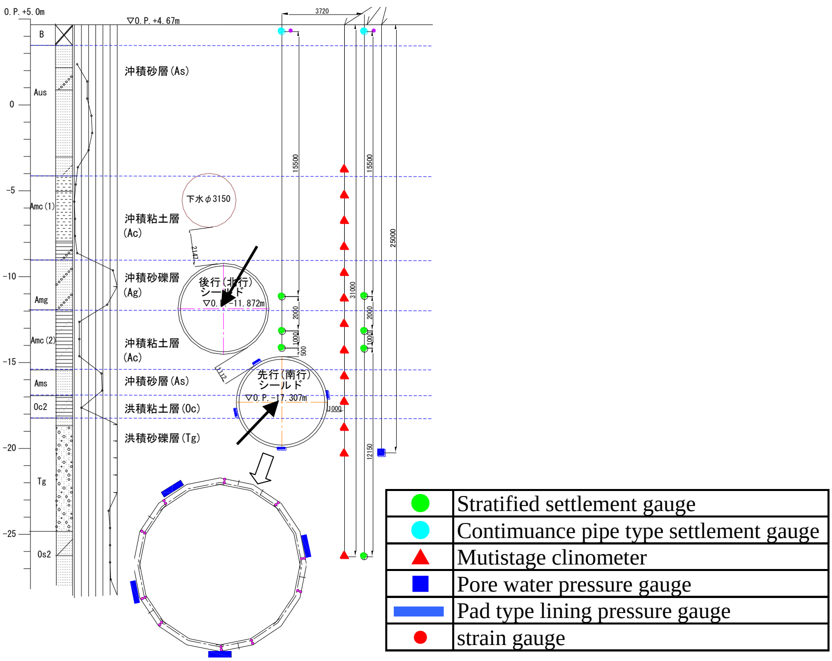


**Figure 1:** Installation position of measurement equipment

**Table 1:** Specification of segments and shield excavation condition

| | | | 1st tunnel | 2nd tunnel |
|---|---|---|---|---|
| Shield excavate type | | | Slurry type | |
| Outer diameter of shield / of tunnel lining(m) | | | 5,44 / 5,30 | |
| Tunnel lining type | | | Cast-iron segment (Width : 0,9 m/ring) | |
| Number of pieces | | | 6 (A-type:3, B-type:2, Key:1) | |
| Young modulus E (kN/m$^2$) | | | $1{,}7 \times 10^7$ | |
| Ares A (m$^2$) | | | 0,0246 | |
| Area moment of intertia (m$^4$) | | | 0,00013 | |
| Overburden pressure (kN/m$^2$) | | | 340 | 240 |
| Cutter face pressure (kN/m$^2$) | Planning value | | 245 | 185 |
| | Monitoring value | | 190 － 280 | 170 － 190 |
| Backfill grouting pressure (kN/m$^2$) | Planning value | | 360 | 280 |
| | Monitoring value | Driving | 100 － 360 | 100 － 300 |
| | | Stopping | 280 － 310 | － |
| Pitching (‰) | Area | | -40,0 － -35,0 | -8,0 － -6,8 |
| | Average | | -35,5 | -7,5 |
| Excavation line shape (vertical) (‰) | | | -33,0 | -10,0 |
| Over cut (mm) | | | 15 | |

# 3 CALCULATION CONDITION

## 3.1 Constitutive Model of Soil

The finite element analyses have been carried out with FEM tij-2D software using an elasto-plastic constitutive model of soils, named subloading $t_{ij}$ model. The constitutive model requires a few soil parameters which can easily be obtained from conventional laboratory tests data. This model can consider influence of intermediate principal stress on the deformation and strength of soils, dependence of the direction of plastic flow on the stress paths, influence of density and/or confining pressure on the deformation and strength of soils.

## 3.2 Load Model considering Construction Loads

The considerable loading factor and the point of view of each construction stage are denoted as follows, and the calculation model for each step is shown in Figure 2.

### 3.2.1 Load model at the arrival of cutter face

When the cutter face pressure is larger than the lateral pressure, thrust acts on the ground consequently heaving occurs above the tunnel. In the reverse situation of the pressure balance, opposite phenomenon happens. Briefly, the ground deformation behaviour depends on the balance between the cutter face pressure and the lateral pressure. In this paper, this influenced ratio is 15% of the differential pressure between both pressures according to reference [4] is applied.

#### 3.2.2 Load model at the first half of shield machine

The ground deformation in this stage significantly depends on the slurry pressure of the cutter face in the additional void between the ground and the shield machine. When the slurry pressure is smaller than the overburden pressure, the settlement occurs just above the tunnel. However, because the slurry pressure is larger than the lateral pressure in the lateral direction, horizontal expansion occurs. Therefore, pressure at the cross section equals to the differential pressure between the cutters face pressure and the ground pressure around tunnel. Moreover, the self-weight of the first half of shield machine without buoyancy force adds pressure on the cross section.

#### 3.2.3 Load model at the second half of shield machine

It has been thought that the influence of backfill grouting pressure is dominant in the ground deformation around tunnel in this stage. But in these monitoring results, the backfill grouting pressure is smaller than the overburden pressure, and it is impossible to heave the ground above the tunnel only by the backfill grouting pressure. Investigating the shield excavation conditions in detail, it is revealed that the thrust to the ground resulting from the difference between the excavation direction and shield machine position is considerably large. Therefore, the cross section pressure equals to the differential pressure between the backfill grouting pressure and the ground pressure around tunnel, the thrust to the ground resulting from the difference between the excavation direction and shield machine position, and the self-weight of the second half of shield machine without buoyancy force.

#### 3.2.4 Load model at the tail passing

Because the backfill grouting pressure is smaller than the overburden pressure in these monitoring results, the settlement occurred again after the tail passed till the cutter face passed. It is proved that the backfill grouting pressure is controlled to the initial balanced condition with ground pressure around tunnel adequately. Therefore, the cross section pressure equals to the differential pressure between the backfill grouting pressure and the ground pressure around tunnel

| Step | Calculating formula | Load model |
|---|---|---|
| 1 step | (arrival of cutter face)<br>$\Delta p_1=(p_{ch}-p_h)*\alpha$<br>$p_{ch}$: cutter face pressure (center)<br>$p_h$: lateral pressure<br>$\alpha$: influence ratio balance between the cutter face pressure and the lateral pressure($\alpha$=0,15) | 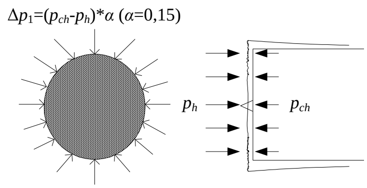 |
| 2 step | (first half of shield machine)<br>$\Delta p_2=p_G+(p_s-p_i)*\beta_1$<br>$p_G$: self-weight of the first half of shield machine without buoyancy force<br>$p_s$: slurry pressure<br>$p_i$: lateral pressure after 1step<br>$\beta_1$:corrected value from 3D to 2D($\beta_1$=0,75) | 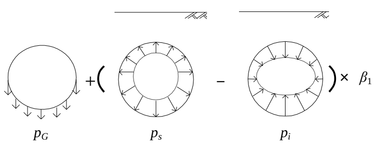 |
| 3 step | (second half of shield machine)<br>$\Delta p_3=p_G+(p_s-p_i')*\beta_2+p_p$<br>$p_G$: self-weight of the first half of shield machine without buoyancy force<br>$p_s$: back fill grouting pressure<br>$p_i$': lateral pressure after 2step<br>$p_p$: pressing load based on the excavation direction and shield machine position<br>$\beta_2$:corrected value from 3D to 2D($\beta_1$=0,25) | 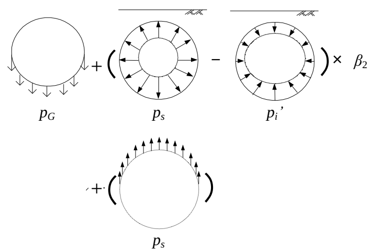 |
| 4 step | (tail passing)<br>$\Delta p_4=(p_s-p_i')*\beta_3$<br>$p_s$:back fill grouting pressure<br>$p_i$':lateral pressure after 3step<br>$\beta_3$:correction factor from 3D to 2D($\beta_3$=0,5) | 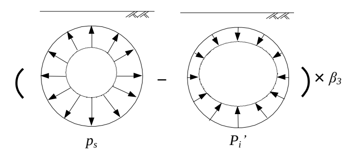 |

**Figure 2:** Illustration of calculation model for ground deformation due to shield excavation

### 3.2.5 Correction factor for transforming 2D condition to 3D condition

This load model considering the construction loads with three dimensional problems is different in each excavation stage. Because the 3D ground deformation is replaced to the 2D problem in this study, correction factors for transforming 2D condition to 3D condition are presumed based on the reference simulating results as Figure 2.

## 3.3 Outline of FE Analysis

Figure 3 shows the finite element mesh. The lateral boundary is extended to the 45-degree influence line from the bottom of the first tunnel, and the lower boundary is configured the twice of shield diameter from the bottom of the first tunnel taking into account the dense sandy layer and stiff clayey layer under the first tunnel. The first tunnel lining is installed immediately after the completion of the first shield exaction and before the excavation of the second shield tunnel.

Soil parameters for elasto-plastic FE analysis are shown in Table 2. These parameters are decided based on the reference [1], because the same elasto-plastic FE program was employed for the braced excavation at the similar ground condition site. Also, the initial stress in the ground is set to become a prescribed over consolidated ground by self-weight consolidation and uniform loading/unloading simulation from the bottom of the ground. Since the excavation time of the shield tunnel is short, about half an hour, the elasto-plastic FE analysis is carried out considering undrained condition.

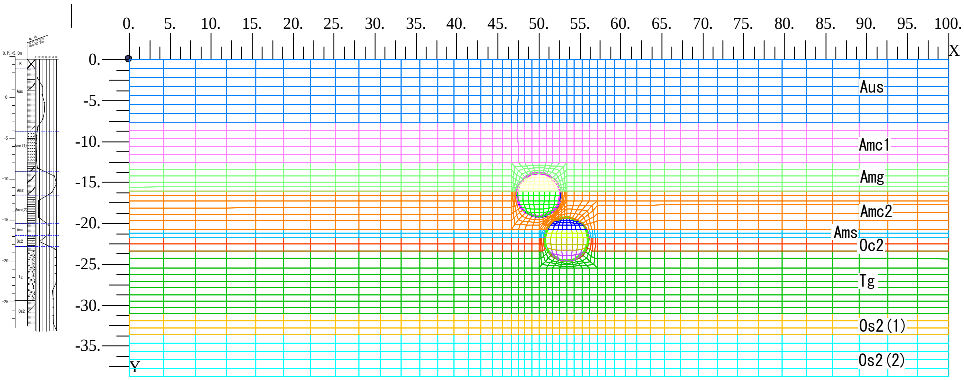


**Figure 3:** Finite element mesh

**Table 2:** Soil parameters for elasto-plastic FE analysis

| Layer | | Lower Depth (GL-m) | SPT N-value (times) | Unit Weight $\gamma_t$ (kN/m$^3$) | Deformation Modulus E (kN/m$^2$) | Poisson Ratio $\nu$ | Soil Parameters for Elasto-plastic FE Analysis (FEM tij-2D) | | | | | | |
|---|---|---|---|---|---|---|---|---|---|---|---|---|---|
| | | | | | | | $\lambda$ | $\kappa$ | N | $R_{cs}$ | $\beta$ | $a_{AF}$ | $a_{IC}$ |
| Holo -cene | Aus | 7.60 | 20 | 18 | 56000 | 0.30 | 0.07 | 0.01 | 0.68 | 3.50 | 1.50 | 200 | 100000 |
| | Amc1 | 12.60 | 0 | 16 | 17745 | 0.45 | 0.16 | 0.02 | 1.23 | 2.25 | 1.57 | 40 | 500 |
| | Amg | 16.10 | 40 | 19 | 112000 | 0.30 | 0.07 | 0.01 | 0.68 | 3.50 | 1.50 | 200 | 100000 |
| | Amc2 | 20.75 | 4 | 17.5 | 31500.0 | 0.45 | 0.25 | 0.04 | 1.50 | 3.55 | 1.70 | 130 | 500 |
| | Ams | 21.70 | 39 | 19 | 107800 | 0.30 | 0.07 | 0.01 | 0.68 | 3.50 | 1.50 | 200 | 100000 |
| Pleisto -cene | Oc2 | 23.40 | 10 | 18 | 43750 | 0.45 | 0.10 | 0.02 | 1.85 | 4.00 | 1.70 | 3500 | 500 |
| | Tg | 31.00 | 90 | 20 | 252000 | 0.30 | 0.035 | 0.0023 | 1.10 | 3.20 | 2.00 | 30 | 500 |
| | Os2-1 | 33.60 | 30 | 18 | 84000 | 0.30 | 0.007 | 0.0005 | 1.10 | 3.20 | 2.00 | 30 | 500 |
| | Os2-2 | 38.70 | 90 | 20 | 252000 | 0.30 | | | | | | | |

## 4 RESULTS AND DISCUSSION

Figure 4 shows the comparison between observed data and calculation results for vertical displacement above the first tunnel and horizontal displacement at a distance of 1m from the first tunnel in each excavation steps. In these figures, FE calculation results with elasto-plastic model and elastic model are illustrated.

At the arrival of cutter face, settlement above the first shield tunnel and expanded horizontal deformation are to some extent in the observed data. On the other hand, the ground movement around first tunnel is insignificant in FE calculation results as the cutter face pressure is balanced with the lateral pressure. This tendency is confirmed in both elasto-plastic and elastic calculation results.

At the first half of shield machine, 4,7mm settlement above tunnel and about 3mm expanding horizontal deformation occur in monitoring data. In elasto-plastic calculation results, about 10mm settlement above tunnel and about 3mm expanding horizontal deformation at spring line of first tunnel are seen. Because the cutter face pressure is smaller than the lateral pressure above the first tunnel, this loading model tends to the stress released condition. Therefore observation and calculation have a good correspondence with this settlement tendency qualitatively. Since the Amc2 layer in FE analysis, which is deposited above the first tunnel, is considered softer than the actual ground condition, calculation settlement is twice of the observational settlement. As a result, the horizontal ground at the right shoulder part of first tunnel mobilizes inside tunnel, and it shows different tendency with the observed data. The settlement trough above the first tunnel of the elasto-plastic calculation indicates local settlement. On the other hand, in the elastic calculation the settlement trough is rather gentle in shape, in short, both settlement troughs show different tendency.

At the second half of shield machine, due to the influence of the thrust to the ground, about 7mm heave and maximum 5mm expanding horizontal deformation occurred in the monitoring ground. The elasto-plastic analysis shows about 4mm heave and maximum 5mm expanding horizontal deformation at the spring line position of the first tunnel corresponding position of the shield machine in the field. The magnitude of the settlement above the shield tunnel is different between the observation and elasto-plastic calculation. But the increment of the settlement between the first half and second half of shield machine in the elasto-plastic FE analysis has quantitatively very good agreement to that of the observed data.

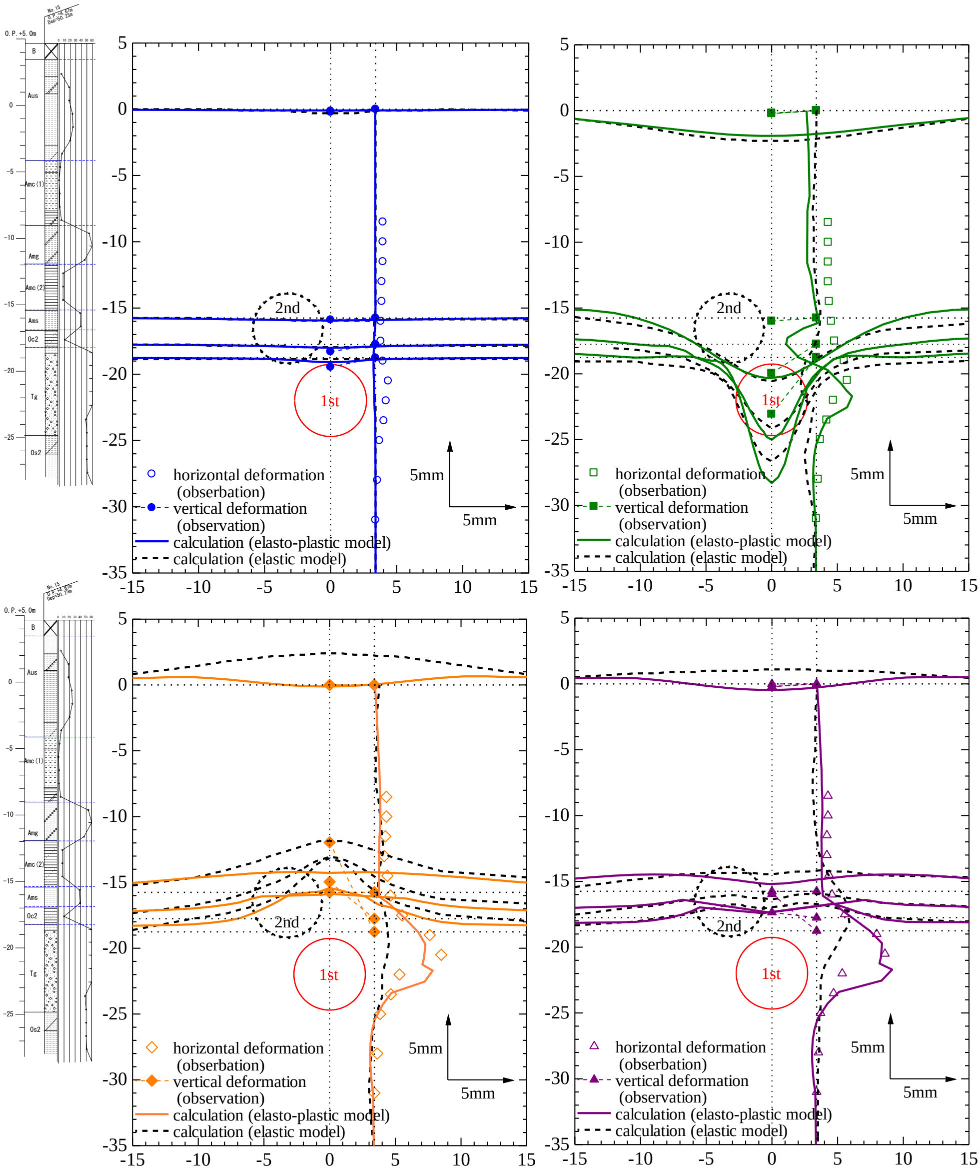


**Figure 4:** Comparison of vertical and horizontal ground deformation between observed data and calculation results for each calculation step

This same tendency is also captured in the distribution of lateral displacement at 1m distance from the tunnel. On the other hand, the elastic calculation results can explain the tendency of the heave above the tunnel and the expanding phenomenon for considering the thrust model based on the shield machine position. However, for instance, the influence of heave extends to the far ground surface, the elastic calculation results are obviously different in comparison to the monitoring results and the elasto-plastic calculation results. Moreover, the heave above the tunnel significantly larger compare to the expanding horizontal deformation, this tendency differs vastly from the observation and the elasto-plastic calculation.

The deformation behaviour at the tail passing is similar to its behaviour at the second half of shield machine. Nevertheless, as the backfill grouting pressure balances with the lateral pressure, the local heave is restricted appropriately and elasto-plastic calculation results have a good correspond with monitoring data in comparison with elastic calculation results.

Figure 5 shows the distribution of the first tunnel lining pressure increment and stress development due to the second shield excavation based on the comparison between observation and elasto-plastic calculation.

At the close part of the first tunnel lining to the second shield excavation, the thrust and the cross section force fluctuate. But there is little change at the opposite part. The elasto-plastic FE analysis perfectly capture the influence of the construction load the same way as observed in the monitoring data. The elasto-plastic FE analysis is able to explain these actual behaviours adequately that cannot be expressed by the analysis using the conventional stress release ratio.

## 5 CONCLUSIONS

In this research, some results can be concluded as follows;

1) The shield excavation is divided four construction process arrival of the cutter face, the first half of shield machine, the second half of shield machine, and the tail passing. The ground movement around shield tunnel are different in each construction steps. Owing to predict the ground deformation behaviour due to shield excavation appropriately with numerical analysis, it is necessary to take into account of the construction load in each construction stage.

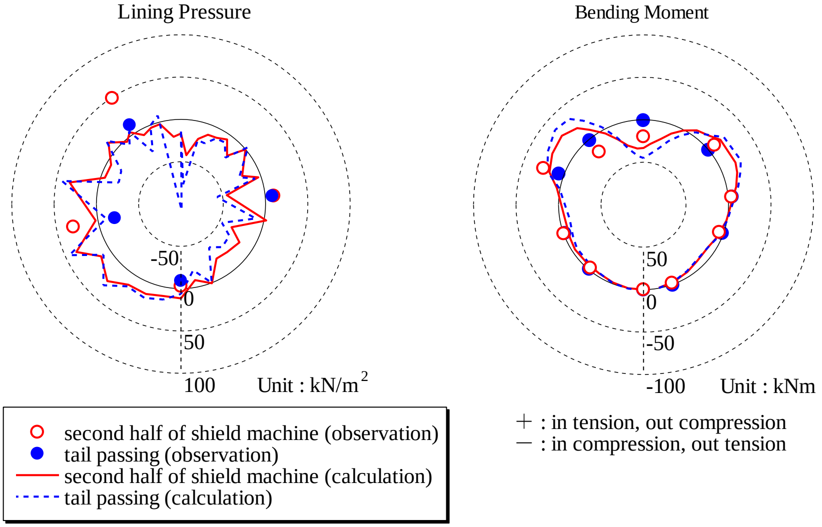


**Figure 5:** Comparison of distribution of earth pressure increment and cross section force of 1st tunnel lining between observed data and calculation results for each calculation step

2) It can be thought that some factors for ground deformation are - i) the balance between the cutter face pressure and the lateral pressure at the cutter face, ii) the balance between the cutter face pressure and the lateral pressure at the first half of shield machine, iii) the differential pressure between the backfill grouting pressure and the ground pressure around tunnel at the second half of shield machine and at the tail passing, and iv) the self-weight of shield machine. Sometime, the thrust associated with the difference between the excavation direction and shield machine positions has an impact to ground deformation.
3) The FE analysis with elasto-plastic constitutive model of soil and the load model considering construction loads is employed to simulate the ground deformation behaviour around tunnel and the nearby tunnel lining pressure and stress development. It is revealed that the elasto-plastic FE analysis is able to explain actual behaviours adequately that cannot be expressed by the analysis using the conventional stress release ratio. Moreover, the elasto-plastic calculation results have a good agreement with the monitoring data in comparison with the elastic calculation results.

## REFERENCES


[1] Konda T., Shahin, H. M. and Nakai, T.: Numerical Analysis for backside ground deformation behaviour due to braced excavation, *9th World Congress on Computational Mechanics and 4th Asia Pacific Congress on Computational Mechanics*, P Antolin et al IOP Conf. Ser.: Mater. Sci. Eng. Vol.10, No.1, 2010.

[2] Nakai, T., Hinokio, M. 2004. A Simple Elastoplastic Model for normally and over consolidated soil with unified material parameters. *Soils and Foundations*, 44(2), pp. 53-70.

[3] Shahin, H. M., Nakai, T, Zhang, F., Kikumoto, M. and Nakahara E., "Behavior of ground and response of existing foundation due to tunneling", *Soils and Foundations*, Vol. 51, No. 3, 2011, pp. 395-409.

[4] Oota H., A. Hashimoto, J. Nagaya and S. Kan: Measurement and consideration of ground deformation due to shield tunnel construction loads, *The Proc. Of Tunnel engineering JSCE*, vol.16, pp.395-402, 2006.